THE ASTROPHYSICAL JOURNAL, 333:305–315, 1988 October 1

EMISSION FEATURES IN *IRAS* LOW-RESOLUTION SPECTRA OF MS, S, AND SC STARS

IRENE R. LITTLE-MARENIN
Air Force Geophysics Laboratory/OPC and Whitin Observatory, Wellesley College
AND
STEPHEN J. LITTLE
Department of Natural Sciences, Bentley College
Received 1988 January 14; accepted 1988 March 29

ABSTRACT

We find a progression of emission features due to dust grains in the 8–22 μm region of *IRAS* low-resolution spectra of MS, S, and SC stars that parallels their increasing C:O ratio and *s*-process enhancement. Strong S stars usually show a 9–14 μm emission feature which peaks around 10.8 μm, whereas mild S or MS stars show a variety of features ranging from the typical 10 μm silicate emission to a three-component feature, to the 10.8 μm S star feature. SC stars show either the S star feature or the SiC feature. A few S stars also show a broad, weak 9–15 μm emission feature. The infrared excesses in the 8–22 μm region correlate very strongly with the period of Mira S, MS, and SC variables (but not for semi regular variables) and increase sharply for Mira variables with periods between 380 and 400 days. The excesses also correlate with mass loss rate for these stars. No 8–22 μm excesses or dust grain emission features are observed for variables including Mira variables with mass-loss rates of $<5 \times 10^{-8}\ M_{\odot}\ \mathrm{yr}^{-1}$.

Subject headings: infrared: spectra — interstellar: grains — stars: carbon — stars: long-period variables — stars: S-type

I. INTRODUCTION

Stellar evolution theory predicts (Iben and Renzini 1983) and observations confirm that M stars evolve to MS → S → (SC) → C stars during the late stages of AGB evolution (Wood 1985) when helium shell flashing occurs and helium-burning products, primarily ^{12}C, *s*-process elements, and technetium are mixed with the outer envelope during the third dredge-up phase. The C:O ratio of stars during the transition changes from $\sim$0.6 (MS stars) (Smith and Lambert 1985) to $\sim$0.8 (S stars) (Smith and Lambert 1986) to $\sim$1.0 (SC stars) (Keenan and Boeshaar 1980; Dominy, Wallerstein, and Suntzeff 1986) and finally to $\sim$1.05–1.1 (C stars) (Lambert *et al.* 1986). At the same time the *s*-process elements are enhanced from solar abundances to as much as 10–100 times solar in the carbon stars (Smith and Lambert 1985, 1986; Smith and Wallerstein 1983; Dominy and Wallerstein 1986; Utsumi 1985). It is estimated that about four to 15 helium shell flashing episodes with subsequent mixing are necessary to change an M star into an S star or SC star (Smith and Lambert 1986; Mathews *et al.* 1986; Winters and Macklin 1987; Wallerstein and Dominy 1988), although some stars may skip over the SC evolutionary phase.

Many late AGB stars lose mass rapidly and develop extensive circumstellar dust shells (CDS). The changing photospheric composition of the AGB stars should be reflected in the composition of the dust grains found in the CDS (Little, Little-Marenin, and Price 1987) since their lost photospheric material passes through the CDS on a time scale of < 1000 yr—a short time compared to the time of 10^4–10^5 yr between He shell flashes (Iben and Renzini 1983).

II. ANALYSIS

IRAS obtained low-resolution spectra (LRS) (*IRAS* Science Working Group 1986) of sources brighter than about 8 Jy in the 8–22 um region in which the emission features of dust grains from silicates at 10 and 18 μm and SiC at 11.2 μm are found. We have analyzed 79 LRS of MS, S, and SC stars to see if their changing photospheric composition produces different emission features. The low-resolution spectrometer scanned simultaneously two wavelength ranges, one extending from 7.7 to 13.4 μm and the other from 11.0 to 22.6 μm. The two spectrum halves in general do not agree at 12 μm *unless* a linear baseline is subtracted, contrary to the information provided chap. 9 of the *Explanatory Supplement to the IRAS Catalogs and Atlases* (1984). The four baseline values are stored as part of the header information for each spectrum or can be calculated by averaging the first and last 20 values of each spectrum half.

In order to study the wavelength dependence of an emission feature, we fit a blackbody energy distribution to the continuum on both sides of an emission feature and subtract this blackbody distribution from the observed spectrum. The temperature of this distribution is representative of the temperature of the CDS and is usually lower than the photospheric temperature. Our procedure allows us to study the spectral characteristics of the emission feature itself. We characterize the strength of the emission feature as the contrast, C_T, which we define as the percentage of the emission above the underlying continuum at the wavelength of maximum emission.

Besides the dust grain emission features, the CDS produces excess continuum emission above the stellar photospheric continuum. We define the total 8–22 μm emission excess, Ex, as the percent of integrated flux in the 8–22 μm region above the photospheric continuum (a 2500 K photospheric temperature was assumed for all stars). Table 1 summarizes our findings. Column (1) gives the most common name (in alphabetical order of their variable star name if applicable) where the prefix CSS refers to the number in Stephenson's (1984) catalog of S stars. C1633 is listed in Stephenson's (1973) catalog of carbon

TABLE 1

MS, S, AND SC STARS

No.	Name (1)	Sp. Class (2)	Var (3)	P	Temp (4)	C_T (5)	feature (6)	Ex (7)	Flx(8) (8)	$M_{\odot}$/yr (9)	% Sil (10)	LRS (11)	Note (12)
	STRONG S STARS												
1	X And	S 3,9e	M	346	1200	--	--	15	18	2.1(-7)		16	
2	BI And	S 8,8	SR	160	2500	--	--	<1	13	4.0(-8)		01	
3	Z Ant	S 5,4	SR	104	520	53	br[11.2]	75	22			42	*
4	W Aql	S 3,9e	M	490	650	16	S(10.8)	57	732	4.5(-6)	70	22	
5	V865 Aql	S 7,5e:	M	365	2500	--	--	< 2	30	4.7(-8)		17	
6	T Cam	S 4,7e	M	373	2500	--	--	< 2	61	5.0(-8)		17	
7	WX Cam	S 5,8	Lb		2500	--	--	<10	7	1.7(-7)		01	
8	BD Cam	S 5,3	Lb		2500	--	--	< 1	64	1.7(-8)		18	*
9	S Cas	S 4,6e	M	612	550	25	S(10.5)	>80	270	2.2(-6)	65	22	
10	U Cas	S 5,5e	M	277	2500:	--	--	< 8	8	4.6(-8)		01	
11	WY Cas	S 6.5pe	M	477	600	30	S(10.8)	55	44	7.5(-7)	50	42	
12	IW Cas	S 4.5,9e	M	396	650	20	S(10.8)	49	45		50	21	
13	TT CMa	S	M	314	650	100	sil.	>97	13			27	*
14	VX Cen	S 8,5e	SR	308	2500	wk	?	5	68			17	*
15	R Cyg	S 4,9e	M	426	750	24	S(10.4)	47	109	6.2(-8)	55	22	
16	AA Cyg	S 7,5	SRb	213	1000	wk	wk	10:	50	8.1(-8)		31	
17	V441 Cyg	S 4,6	SRa	375	1200	wk?	--	13	12	4.2(-8)		16	
18	R Gem	S 5,9e	M	370	800	--	--	20	29	1.4(-7)		16	
19	DY Gem	S 8,5	SRa	1145	700	34	S(11:)	42	22	1.1(-7)	45:	42	
20	pi^1 Gru	S 5,7e	SRb	150:	750	28	S(10.7)	43	993		50:	42	
21	R Lyn	S 4,7e	M	379	2000	27	S(10.5)	10	26	6.2(-8)	--	16	
22	SU Mon	S 3,6	SRb		2500:	23	S(10.9)	9	24	6.3(-8)	30	18	
23	V521 Oph	S 5,4	SRb	320	3500	--	--	< 8	51	4.5(-8)		17	
24	RZ Sgr	S 4,4ep	SRb	223	700	wk	--	35	41			16	
25	ST Sgr	S 5,5e	M	395	1000	23	S(10.8)	30	58	9.5(-8)	60	21	
26	ST Sco	S 4,6	SRa	195	800	24	br[11.6]	30	57	6.6(-8)		16	*
27	V635 Sco	S 7,6	Lb		2500	--	--	< 3	18			17	
28	UU Vel	S 7,8e	M	409	1500	60:	S(11:)	20:	14		35:	01	
29	EP Vul	S 6,5	Lb		900	25	11.2	20	37	6.5(-8)		16	*
30	HD 191630	S 4,4	-------		2500	--	--	< 2	15			18	
31	BD-38°4770	S 4,6	-------		1000	22	SiC	20	15			16	*
	MILD S and MS STARS												
32	W And	S 6,1e	M	396	950	23	3 comp	31	187	2.7(-7)		22	
33	RW And	S 6,2e	M	430	750	?	?	53	39	2.3(-7)		22	*
34	NO Aur	M2SIab	Lc		800	37	S(10.8)	39	43		50		
35	RS Cnc	M6IIIaSe	SRc	120:	1000	30	sil.	32	415			22	
36	V365 Cas	S 7,2	SRb	136	1200	28:	S(10.5)	20	24	7.9(-8)	60:	16	
37	T Cep	M 6.5e	M	388	800	11	br[11.3]	32	869			15	
38	T Cet	M5-6SIIe	SRc	159	700	wk?	--	22	220			16	
39	W Cet	S6,3-9,2e	M	351	1000	--	--	7	16	3.3(-8)		16	
40	TV Dra	M6p(S)	Lb		800	9	br[11.3]	27	66	7.1(-8)		15	
41	S Her	M6(S)e	M	307	2500	--	--	< 3	45			17	
42	ST Her	M6-7IIIaS	SRb	148	650	14	S:(11:)	33	209		35:	41	
43	OP Her	M5IIb(S)	SRc	121	3500	--	--	< 1	80			17	*
44	R Hya	M6.5(S)e	M	389	760	11	br[11.4]	35	2068			15	
45	Y Lyn	M6SIb-II	SRc	110	950	37	S:(10.3)	40	135		90	23	
46	RR Mon	S 7,2e	M	393	800	30:	3 comp	41	19	1.5(-7)		16	
47	4o^1 Ori	M3.2IIIaS	SRb	30:	2500	--	--	< 1	113			18	*
48	HT Per	M6(S)	SR:	128:	600	27	S(10.5)	50	17		50:	15	
49	SU Pup	S 4,2e	M	340	800	30	3 comp	43	15			22	
50	RT Sco	S 7,2	M	449	700	20	3 comp	52	174			22	
51	DK Vul	S 4,2	SRa	370	800	?	?	16	19	1.6(-7)		16	*
52	HD 35155	S 4,1	-------		2500	--	--	< 6	10	2.9(-8)		16	
53	HD 49683	M4S	-------		3000	--	--	< 6	8	3.0(-8)		16	
54	HD 92681	S 5,2	-------		2500	--	--	< 1	13			18	
55	HD 110994	S 5,1	-------		3500	--	--	< 3	21			17	
56	HD 118685	S 6,2	-------		2500	--	--	< 2	34			18	*
57	BD-36°4827	S 5,2	-------		3500	--	--	< 2	12			18	
	SC STARS												
58	R CMi	SC5/10=C5,1	M	338	3500	50:	SiC:	15:	16			01	
59	UY Cen	SC6/8	SR	115	1200	23	S(11:)	9	63		35	43	*
60	AM Cen	SC	Lb		2500	v.wk	?	2	20			18	*
61	S Lyr	SCe	M	438	630	20	S(10.9)	42	54		45	41	*
62	FU Mon	C8,0J;CS	SR	310	4000	--	--	< 1	21			18	*
63	GP Ori	C8,0J,SC	SRb	370:	2500	--	--	<10	12			17	
64	CSS 788	SC;S5,8	---	---	3500	--	--	< 3	24			18	

TABLE 1—*Continued*

No.	Name (1)	Sp. Class (2)	Var (3)	P	Temp (4)	C_T (5)	feature (6)	Ex (7)	Flx(8) (8)	$M_☉$/yr (9)	% Sil (10)	LRS (11)	Note (12)
	S STARS WITH LITTLE INFORMATION												
65	CSS 861	S			540	57	non S	52	15			15	*
66	CSS 929	Se			600	22	S(10.8)	51	60		50	42	
67	CSS 975	S			2500	45:	br[11.4]	20:	15			15	*
68	CSS 1011	S	var		800	30:	S:(10.9)	26:	8		40:	01	
69	CSS 1043	Se			1000	28	3 comp:	26	21			16	
70	CSS 1146	S			380	140	sil	>290	32			29	*
71	CSS 1259	S			375	97	sil	>210:	6			28	
72	C 1633				850	25	3 comp	36	45			22	*
	SPECTROSCOPIC MS STARS												
73	CU Dra	M3III	Lb:		3000	--	--	0	92	=BS 5226		18	
74	NZ Gem	M3II-IIIS	SR		3500	--	--	0	36	=BS 2967		18	
75	DE Leo	M2IIIabS	SRb		4000	--	--	<12	25	=BS 4088		01	*
76	GZ Peg	M4IIIS	Lb?		3500	--	--	0	124	=BS 8815		18	
77	BS 2508	M2IIIS	-------		3000	--	--	0	42			17	
78	BS 7442	M5IIIaS	-------		3000	--	--	0	31			17	
	M STAR												
79	RT Aql	M6eS	M	327	620	24	sil	42	83			24	*

NOTES.—Asterisk indicates a note to a specific star, given below by row number. Colon (:) indicates an uncertain value; wk indicates a weak feature. For col. (6), sil = 10 μm silicate feature; br = broad 9–15 μm feature; S = 10.8 μm S star feature.

Notes to stars indicated by asterisk in col. (12):

3 Z Ant: noisy; broad feature; max at 11.2 μm and weak peaks at 10 and 13 μm
8 BD Cam = BS 1105, excess shortward of 9.5 μm
13 TT CMa: no 18 μm emission feature
14 VX Cen: weak broad 9.5–16 μm emission feature
16 AA Cyg: weak, broad emission feature
26 ST Sco; broad 9.5–15 μm emission feature
29 EP Vul: emission feature with peaks at 11.3 and 13 μm; not SiC
31 BD −38°4770: emission matches 11.3 μm SiC feature; may be C star?
33 RW And: possible self-absorption at 10.5 μm
43 OP Her = BS 6702
47 $4o^1$ Ori: emission excess shortward of 9.5 μm
51 DK Vul: possible 9.5–15 μm emission or possible 9.5 μm absorption feature
56 HD 118685: emission excess shortward of 9.5 μm
59 UY Cen: absorption feature at 14 μm, probably due to C_2H_2 and HCN
60 AM Cen: very weak emission feature is present
61 S Lyr: LaO absorption at 0.74 and 0.79 μm; possibly an S star
62 FU Mon: possible C_2H_2 and HCN absorption feature at 14 μm
65 CSS 861: asymmetric 9–14 μm emission feature with peak at 10.4 μm
67 CSS 975: broad 9.5–15 μm emission feature
70 CSS 1146: late M, not S
72 C 1633: classified as C star; emission feature more typical of MS stars
75 DE Leo: emission excess shortward of 9.5 μm
79 RT Aql: no ZrO, no Tc (Little-Marenin, Little, and Bauer 1987): probably M star

stars; however, its LRS spectrum does not show an SiC feature but instead a three-component feature, and we assume it to be an MS star. Columns (2) and (3) give the spectral type, variability class, and period as listed in the *General Catalog of Variable Stars* (*GCVS*) (Kholopov 1985), Wing and Yorka (1977), or the *Yale Bright Star Catalog* (Hoffleit and Jaschek 1982). Column (4) lists the derived temperature of the continuum underlying emission features (if present) in the 9–14 μm region. For about 80% of the stars with emission features the temperature lies between 600 and 1000 K. At times, more than one temperature is needed to characterize the CDS which produces the 8–22 μm emission excesses, a hotter temperature ($T > 1500$ K) for the 8–9 μm region, and a cooler temperature ($T < 500$ K) for the 14–22 μm region. Column (5) lists the contrast, C_T, of any emission feature, and column (6) gives the type of feature observed and, in parentheses, the wavelength of peak emission. The various types of emission features, such as "S" for the most common S star feature, the three-component feature, and a broad (br) 9–15 μm emission feature are discussed in greater detail below. "Sil" refers to the 10 μm silicate emission feature observed in the LRS of M stars and SiC refers to the 11.2 μm feature observed in C stars. Dashes in columns (5) and (6) indicate no emission feature is observed, and a question mark (?) indicates an emission feature that is difficult to characterize. Column (7) lists the emission excess, Ex, above the photospheric continuum in the 8–22 μm region. In column (8) we list the flux in janskys at 8 μm as measured in the LRS, since Gal *et al.* (1987) suggest that the strength of the 10 μm silicate emission feature in M variables correlates with the flux at 8 μm, i.e., that the more distant stars [lower F(8 μm)] selectively show the stronger emission features. No such correlation appears to exist for the S, MS, and SC stars except that, as expected at low flux levels, F(8 μm) < 20 Jy, only the stronger emission features with $C_T > 20$% are detectable above the noise. Column (9) lists the mass loss rates as calculated by Jura (1988); column (10) gives the percentage of 10 μm silicate emission needed to match the observed S star dust grain feature (discussed below). Column (11) lists the LRS characterization defined in chap. 9 of the *Explanatory Supplement to the IRAS Catalogs and Atlas* and in part defined below. An asterisk in column (12) indicates a remark at the end of Table 1.

We will exclude from the rest of the discussion the six stars listed in Table 1 as spectroscopic MS stars as defined in Little, Little-Marenin, and Bauer (1987). These stars show neither enhanced *s*-process abundances nor Tc (Smith and Lambert 1986; Little, Little-Marenin, and Bauer 1987). They are likely to be misclassified M stars, or their MS classification, if correct, is most likely produced by unusual atmospheric conditions. Their LRS are typical of nonvariable or low-amplitude early (<M4) M stars with no indication of a CDS, i.e., no emission features are visible, and their 8–22 μm fluxes are extensions of their photospheric fluxes ($T \approx 2000$–4000 K). RT Aql is also excluded from the discussion since it is most likely a misclassified M star and not an MS star. It has no Tc, and Keenan, Garrison, and Deutsch (1974) observed no ZrO. Its LRS shows the typical 10 and 18 μm silicate emission features found in many variable M stars.

About one-third of the remaining 72 spectra show only a smooth 8-22 μm continuum which can, for most stars, be matched with a 2000–3000 K blackbody energy distribution representative of the photospheric temperatures of these stars. The other two thirds of the spectra show emission features of weak to moderate strength. As expected from the studies of M stars, we find that seven out of the eight nonvariable S and MS stars have featureless photospheric continua. Only BD $-38°4770$ shows a definite emission feature probably due to SiC. It is the only known S star with a pure SiC emission feature and needs to be investigated further to see whether it is a misclassified C or SC star. It also may be an unrecognized variable star even though *IRAS* estimated only a 12% probability of its being variable in the infrared, similar to the probabilities observed for the other non-variable stars. Unexpectedly, four out of 23 (17%) S, MS, and SC Mira variables show *no* emission features and no 8–22 μm excesses. These are V865 Aql (S7,5e:, $P = 365^d$), T Cam (S4,7e, $P = 373^d$), U Cas (S3,5e, $P = 277^d$); and S Her [$M6$(S), $P = 307^d$]. A few other stars show a cooler, featureless continuum including the two Mira variables, X And (S3,9, $P = 346^d$, $T = 1200$ K) and R Gem (S3,6, $P = 370^d$, $T = 800$ K) in which a small infrared excess is present but no dust grain emission feature is observed. Hence, stars with featureless continua include all types of stars from the nonvariables to the Mira variables.

III. DISCUSSION

The S, MS, and SC stars can be divided into three groups: (1) 20 stars with featureless 2000–4000 K photospheric continua in the 8–22 μm region (discussed above); (2) a few stars with featureless continua and cooler than photospheric temperatures (T between 1200 K and 700 K) in the 8–22 μm region; and (3) 45 stars with emission features. A few stars defy the above classification scheme and are discussed in the remarks to Table 1.

The *IRAS* low-resolution spectra are characterized according to the shape of their energy distribution and type of emission and absorption features observed in the 8–22 μm region. Spectra with typical oxygen-rich silicate dust grain emission features extending from 8 to 14 μm with a maximum around 10 μm are characterized as $2n$, where $n = 1$–9 measures the strength of the 10 μm emission. Many also show the 18 μm emission due to the bending mode of silicates. Spectra with a carbon-rich, SiC dust grain emission feature extending from 10 to 14 μm and a maximum at 11.2 μm are characterized as $4n$, where $n = 1$–9 measures the strength of the SiC feature. No other dust grain emission features were recognized in the LRS characterization since none were known. Among the S, MS, and SC stars, we find three additional types of weak emission features: (1) an emission feature extending from 9 to 14 μm that peaks in general around 10.8 μm but the maximum can vary from 10.3 to 11 μm; (2) a three-component feature extending from 9 to 14 μm with peaks at 10 μm, 11 μm, and 13.1 μm (Little-Marenin, Little, and Price 1986); and (3) a broad, weak 9–15 μm emission feature with a poorly defined maximum around 11.4 μm. None of these three features match the narrower (smaller FWHM) spectral characteristics of the typical silicate or SiC emission. An LRS characterization of $1n$ is used to indicate a blue featureless spectrum with $n = 1$–9 being 2 times the spectral index. Hence, spectra characterized as 17 and 18 should show only a photospheric continuum and spectra characterized as 16–12 should show a smooth cooler temperatures continuum. However, for variable stars, we find that only spectra characterized as 18 or 17 show, with few exceptions, no emission features, whereas over 50% of all the other spectra characterized as $1n$ tend to show various types of weak, broad emission features. Chapter 9 in the *Explanatory Supplement to the IRAS Catalogs and Atlases* (1984) gives a complete discussion of the 10 different classes. A look at Table 1, columns (9) and (11), indicates that the LRS characterizations are not able to identify the weak, broad emission features we observe.

a) The 10.8 Micron S Star Feature

The emission features found in the spectra of S stars in general are weak with an average contrast, C_T, of about 27%. In strong S stars, those with abundance classes between 4 and 9 (i.e., Sx, 4, to Sx, 9), emission features peak between 10.3 and 11 μm and have a FWHM value of about 2.4 μm. We will refer to this feature as the S star feature, and we list its wavelength peak in Table 1, column (6) and its LRS characterization in column (11). Most of these spectra are characterized as 21–23 and 41–43 depending on the exact wavelength peak of the feature. Thomas, Robinson, and Hyland (1976) noted this S star feature in the spectrum of π^1 Gru. The LRS of S Cas (S4,6) (Fig. 1) illustrates a typical spectrum of this type. The top panel shows the observed spectrum, a 550 K blackbody energy distribution fitted to the continuum underlying the emission feature, and the difference spectrum (observed − blackbody) plotted along the wavelength axis. We know of no laboratory spectrum of grains that produces the S star emission feature. However, Gehrz *et al.* (1984) noted an emission feature in Nova Aquilae 1982 with a peak at 10.5 μm. The shape of the Nova Aquilae emission feature appears to be similar to that of S stars. The high abundances of heavier elements in the nova (Snijders *et al.* 1984) suggests that both the S star and the Nova Aquilae feature are produced under similar conditions in CDS and/or by the same carrier. We find it unlikely that the feature is due to SiC as suggested by Gehrz *et al.* (1984) or due to silicates as suggested by Bode *et al.* (1984) since the wavelength dependence of the Nova Aquilae emission feature agrees with neither (see Figs. 5 and 6 in Gehrz *et al.*). It is possible that silicates combined with an *s*-process element such as Ba, Zr, etc. may be responsible for the feature in both the S stars and Nova Aquilae. Unfortunately no *s*-process elemental abundances could be determined for Nova Aquilae. On the other hand, we find that the feature observed in S star LRS spectra can be modeled reasonably well by a co-addition of the 10 μm silicate feature and the 11.2 μm SiC feature. The percentage of silicate emission necessary to produce the co-added feature varies from star to star but tends to lie in the 50%–70% range and is listed in Table 1, column (10). The percent of SiC equals 100 minus the percentage of silicate. This simple co-added model fits the width of the feature reasonably well but is less able to

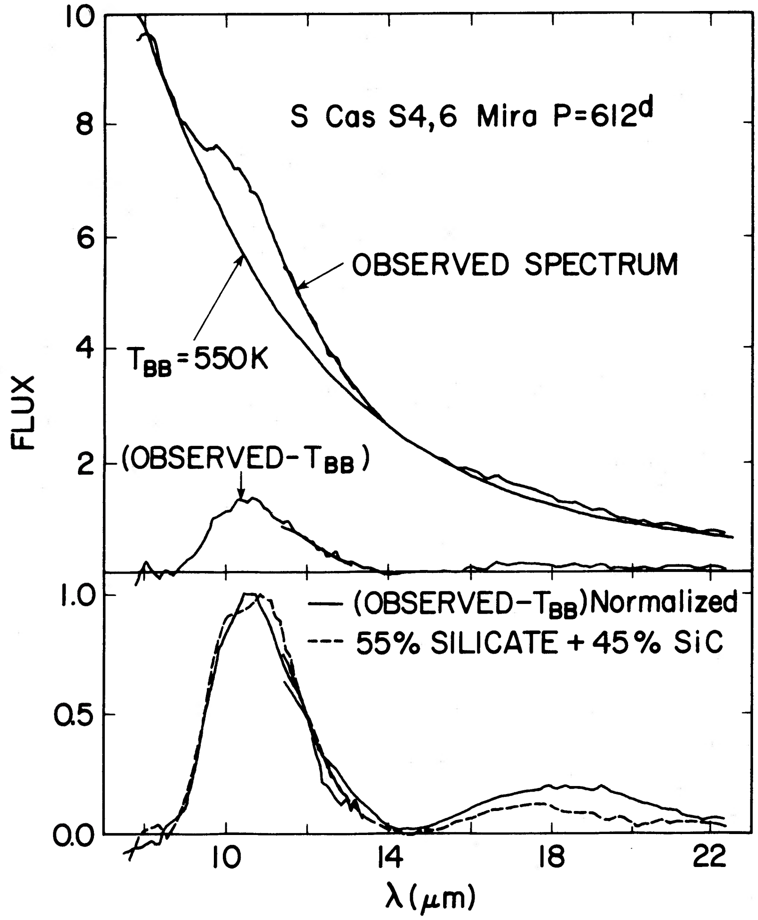

FIG. 1.—The observed spectrum of S Cas is matched with a 550 K blackbody energy distribution (*top panel*). The difference spectrum (observed − blackbody distribution) is plotted along the wavelength axis. The emission feature is typical of the S stars. The normalized difference spectrum is matched with a blend of 55% silicate + 45% SiC (*bottom panel*).

reproduce the smooth emission peak observed in S stars as can be seen in the bottom panel of Figure 1 where the normalized emission feature of S Cas is well modeled with a combined feature of 55% silicate and 45% SiC. It is unclear whether the co-addition of silicate and SiC emission is a valid characterization of the S star feature; it is usually assumed that SiC and silicate dust grains cannot co-exist in chemical equilibrium in the CDS.

Wing and Yorka (1977) argue that surveys of S stars and MS stars are incomplete based on their analysis of IRC (Neugebauer and Leighton 1969) S stars since it is possible ZrO bands were absent on the date of observation or were missed on objective prism plates. Hence, we have collected in Table 2, 26 variable stars which show the 10.8 μm S star feature but are classified as M stars. These stars should be reinvestigated in order to see if the presence of the 10.8 μm feature can be used as a classification criterion for S stars.

b) *The Three Component Feature*

Some of the S stars with emission features and abundance classes of 1 to 2 (stars in the Sx, 1 class are also referred to as MS stars) show a three-component feature with peaks at 10 μm, 11 μm, and weakly at 13.1 μm and in some cases a longer wavelength feature that peaks around 19 μm. The intensities of the components relative to each other vary, but in general the ratio of the 10 to 11 μm feature lies between 1.0 and 1.4. These

TABLE 2

STARS WITH THE 10.8 S STAR FEATURE

Name	Spectral Class	F(8 μm)
V Aps	M8	29
V429 Aql	M2–M6	19
W Aqr	M6e	56
SV Aqr	Mb	52
W Ara	M5 III	29
UX Ara	...	30
VY Cas	M6–M7	34
VX Cep	M8	41
V405 Cyg	M6.5	42
V702 Cyg	M5	23
V Eri	M6 II	238
AM Gem	M10	15
S Gru	M8 IIIe	103
FZ Hya	M6	77
SV Lib	...	38
RS Lyn	M7	33
EW Peg	M6	14
AE Per	M5	25
GH Per	M6.5	49
R Psc	M3e–M6e	25
Y Pup	M7	43
SU Sgr	M6	129
V1692 Sgr	M9	22
V Tel	Mc	95
SU Vel	Mc	145
SZ Vel	M5e	40

spectra, usually characterized as 16 or 22 in the LRS catalog, are clearly different from the 10 and 18 μm silicate emission features found in many M star spectra. The short-wavelength side of the three-component feature is similar to the M star 10 μm emission but shows considerably more emission longward of 10.5 μm with a FWHM (three-component = 2.7 μm as compared to a FWHM (10 μm) = 2 μm. In contrast, the 18 μm silicate feature is broader (FWHM = 5.4 μm) than the 19 μm feature (FWHM = 4.4 μm), but it is possible that we underestimate the width of the 19 μm emission since the feature is weak and the LRS do not extend beyond 22 μm. Whether or not the three-component and the 19 μm feature are produced by a dust grain of differing composition and/or a different size distribution is not yet known. MgSiO annealed *in vacuo* can show structure around 10 μm at times with additional components at 9.2 and 11.2 μm (Nuth, Donn, and Nelson 1986). Since the three-component feature shows no peak at 9.2 μm, we are probably not observing annealed MgSiO. However, it is possible that a similar process operating on a different compound produces the three-component feature. Figure 2 shows the three-component feature in the LRS spectrum of RT Sco (S7, 2) matched with a 700 K blackbody energy distribution. The difference spectrum is plotted along the wavelength axis. The bottom panel of Figure 2 shows the composite three component feature of several Sx, 1 and Sx, 2 stars. It is very similar to the three-component feature found in about 15% of the M stars with emission features (Little-Marenin, Little, and Price 1986). Since weak ZrO bands in MS stars can be missed on objective-prism spectra, it is possible that all M stars with three-component features are unrecognized MS stars.

c) *The Broad 9–15 Micron Feature*

The three S stars, Z Ant, V635 Sco, and CSS 975, show a broad 9–15 μm emission feature. The poorly defined peak tends to have a maximum around 11.4 μm and these features are identified as "br" in Table 1, column (6) with the wavelength peak enclosed in square brackets. Roughly 30%–40% of variable M stars with an LRS characterization of 14, 15, and 16 show this broad, weak type of emission.

IV. MS STARS AND SC STARS

Of the 26 MS stars listed in Table 1, only RS Cnc has a pure 10 μm silicate emission feature. Four other stars show various versions of the three-component feature, five show the S star feature and three the broad 9–15 μm feature. Most of the rest of the stars have featureless continua which are matched with

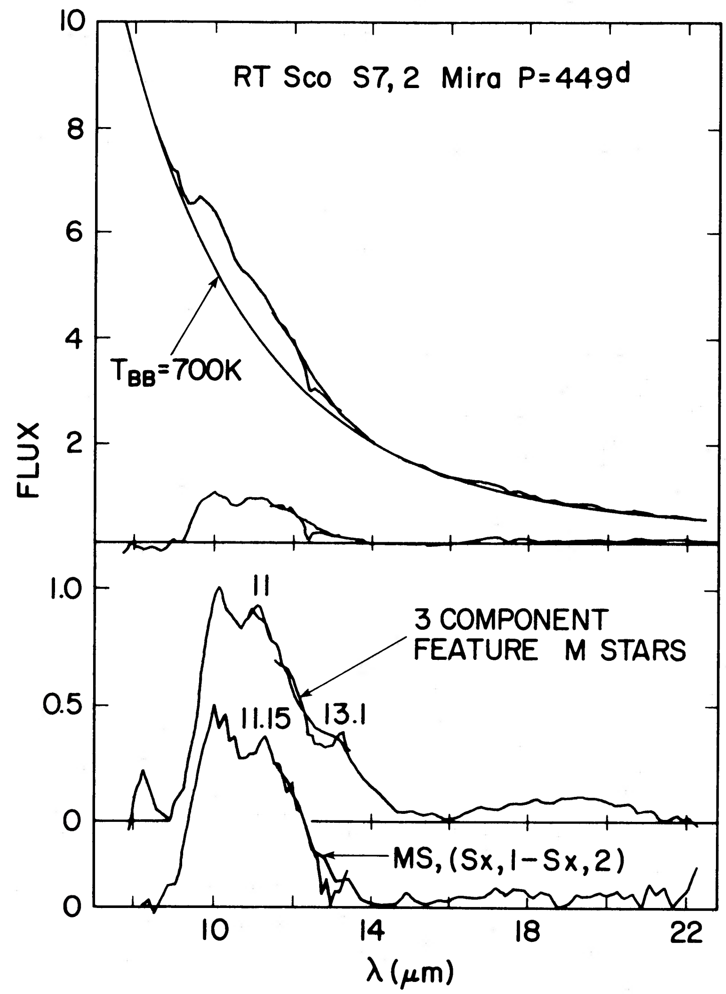

FIG. 2.—The observed spectrum of RT Sco is matched with a 700 K blackbody energy distribution (*top panel*). The difference spectrum (observed − blackbody energy distribution) is plotted along the wavelength axis. In the bottom panel the average three-component feature with peaks at 10, 11, and 13.1 μm observed in some M stars can be compared to the very similar three-component feature observed in mild S and MS stars.

photospheric temperatures with the exception of T Cet. Its spectrum shows an excess longward of 9 μm, but no distinct emission feature.

It appears that the dust grain emission features found in MS stars span the range of features found among the M and S stars. Since M stars evolving to MS and S stars are estimated to be AGB stars experiencing the third dredge-up, which produces an increase in *s*-process elements and carbon, we suspect that the observed range of dust grain emission features in the CDS of MS stars is related to the change in the photospheric composition of the parent star.

Among the seven SC stars listed in Table 1, we find three (FU Mon, GP Ori, and CSS 788) show a photospheric continuum, and another three stars show emission features. AM Cen is not discussed because a weak emission feature may be present in this noisy spectrum but is too weak to classify accurately. In Figure 3 we plot the observed LRS of S Lyr, UY Cen, and R CMi along with blackbody energy distributions representative of their underlying continua and their difference spectra. The normalized difference spectra of the three SC stars are overplotted with different C star emission features (*bottom panels*). S Lyr and UY Cen show the 10.8 μm S star feature which can be matched by a 45% and 35% silicate plus 55% and 65% SiC feature, respectively (Figs. 3*a* and 3*b*, *bottom panels*). In addition the spectrum of UY Cen is best understood as also having an absorption feature around 14 μm (Fig. 3*b*) attributed in some C stars to C_2H_2 and HCN by Willems (1987). Similarly, FU Mon appears to show the C_2H_2 and HCN absorption feature but no emission feature. The apparent 8–9 μm emission feature seen in S Lyr (Fig. 3*a*, *bottom line*) is an artifact because we assumed a single temperature for the CDS in the 8–22 μm region. A temperature of 2500 K is needed to fit the 8–9 μm region and a temperature of 640 K to fit the 10–22 μm region. S Lyr appears to be more closely related to the S star since no obvious C star characteristics are present and Catchpole and Feast (1971) find that ZrO is stronger in the spectrum of S Lyr than in UY Cen. UY Cen shows both S star and C star characteristics. R CMi may have a nearly pure SiC emission feature (Fig 3*c bottom panel*) seen in C star LRS, but its spectrum is very noisy, and it is difficult to be certain. R CMi also has been classified as a marginal carbon star.

As found for the MS stars, the emission features observed in

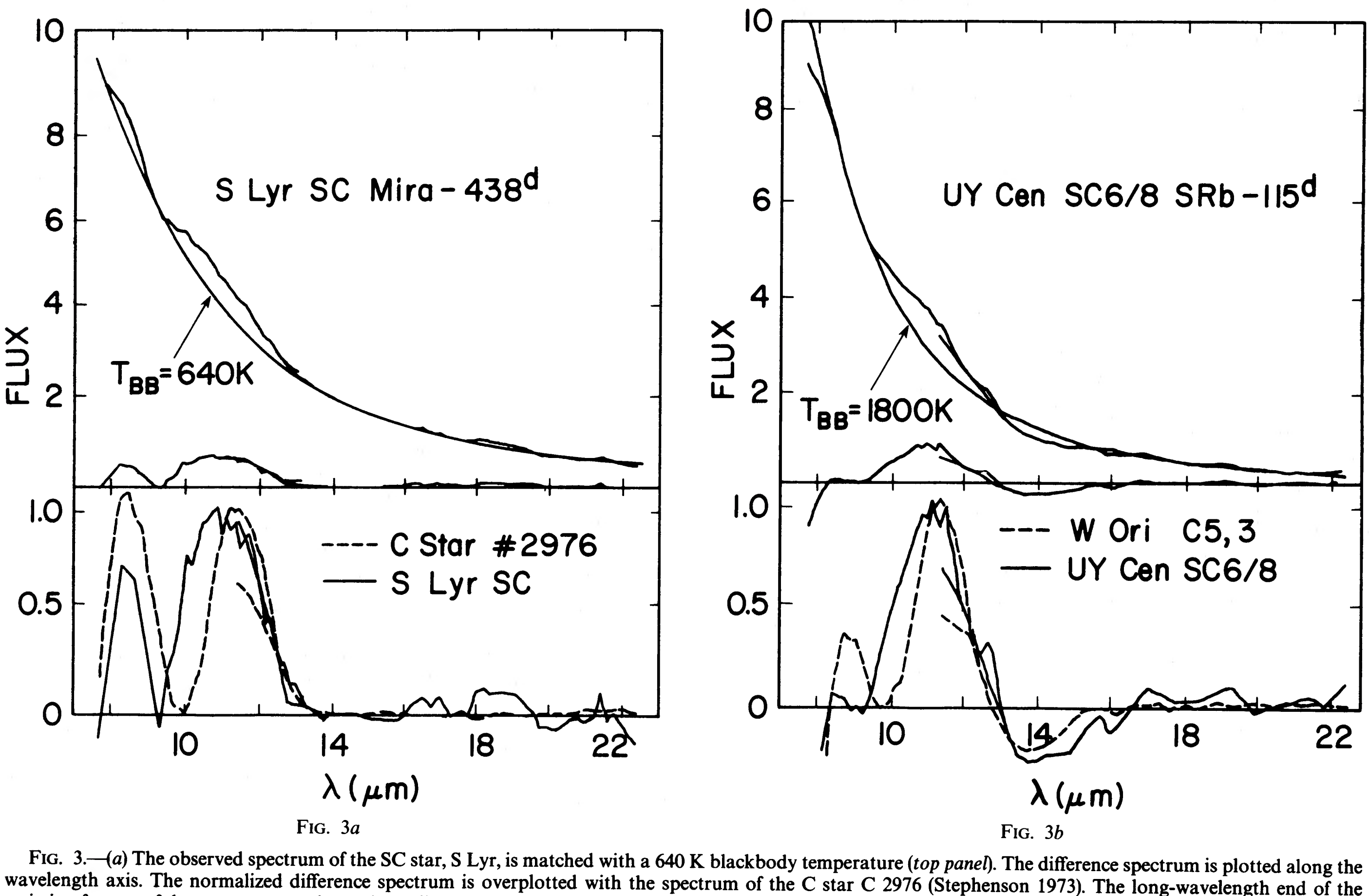

FIG. 3*a* FIG. 3*b*

FIG. 3.—(*a*) The observed spectrum of the SC star, S Lyr, is matched with a 640 K blackbody temperature (*top panel*). The difference spectrum is plotted along the wavelength axis. The normalized difference spectrum is overplotted with the spectrum of the C star C 2976 (Stephenson 1973). The long-wavelength end of the emission feature of the two stars matches quite well. However, the short-wavelength side of the feature can be matched by co-adding a silicate and an SiC feature. (*b*) The observed spectrum of UY Cen is matched to an 1800 K blackbody energy distribution (*top panel*). The difference spectrum is plotted along the wavelength axis. The normalized difference spectum of UY Cen is overplotted with the difference spectum of W Ori. A contribution of possible silicate emission to the spectrum of UY Cen at the short-wavelength side can be seen. An additional absorption feature around 14 μm, atributed to C_2H_2 and HCN, can be seen in both spectra. (*c*) The observed spectrum of R CMi (smoothed over five points) is matched with a 3500 K blackbody energy distribution. The difference spectrum is plotted along the wavelength axis. The difference spectrum (smoothed over three points) is overplotted with an average SiC feature calculated from many C star spectra. The two features match reasonably well. No additional emission at the short-wavelength side of the feature (as is observed for the S stars) appears to be present.

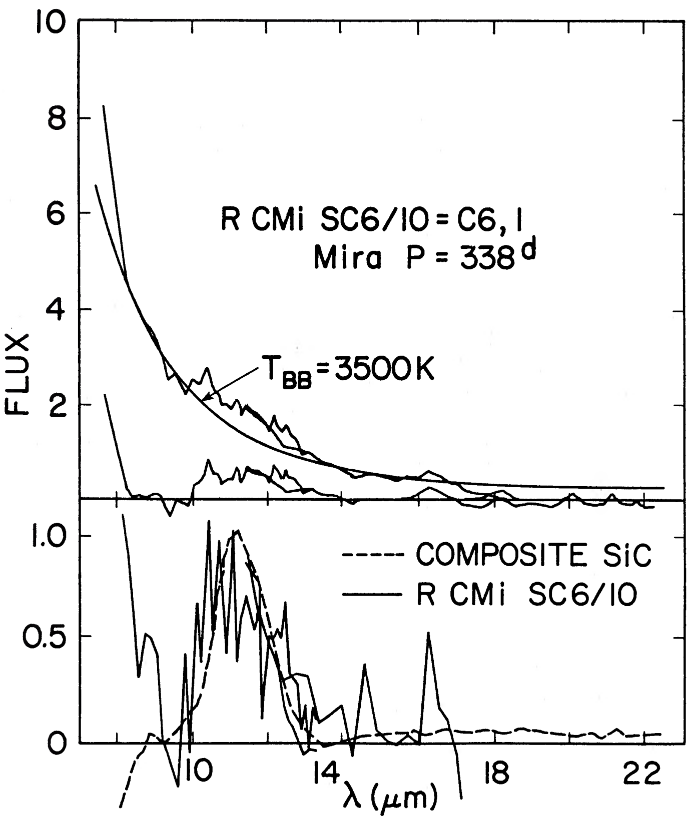

FIG. 3c

SC star spectra may reflect the changing photospheric composition of stars evolving to C stars. We have not distinguished between SC and CS stars.

V. STARS WITH STRONG 10 MICRON EMISSION

TT CMa, CSS 1146, and CSS 1259 have very strong 10 μm silicate emission features with a contrast C_T of 100%, 140%, and 100%, respectively, which is atypical of the other S stars. CSS 1146 appears to be incorrectly listed as a S star in Stephenson's (1984) catalog. Its spectrum appears to be late M (Allen *et al.* 1977; P. Pesch, private communication). Nothing unusual is known about the two other stars; both TT CMa and CSS 1259 show LaO bands on objective prism plates. In *IRAS* color-color plots (see, for example, Zuckerman and Dyck 1986), TT CMa and CSS 1259 are located among the M stars and not among the other S stars suggesting that their CDS are more characteristic of the oxygen-rich material of M stars than of the material located around S stars. It is possible that these two objects are binary stars with components close in mass, as has been suggested for the C stars which show very strong 10 and 18 μm emission features in their LRS (Benson and Little-Marenin 1987; Little-Marenin, Benson, and Little 1987; Little-Marenin, Benson, and Dickinson 1988). The silicate emission is hypothesized to come from an M star with a CDS which depresses its visible light so that the S star is predominant in the visible and near infrared region. Since the spectra of M and S stars are very similar in the 2–5 μm region, it will be very difficult to spectroscopically distinguish between an M and S star component in 2–5 μm spectral range where the crossover in flux between the S star and the M star component is estimated to lie.

VI. PERIOD VERSUS 8–22 MICRON EXCESS

We searched for a correlation between the infrared 8–22 μm excess of S, MS, and SC Miras and their period. We defined the 8–22 μm excess as the percent of integrated flux in the 8–22 μm region that lies above the estimated photospheric continuum and is listed in Table 1, column (8). We assumed a 2500 K photospheric temperature for all the stars since in the 8–22 μm region the shape of the blackbody energy distribution varies very little for all $T > 2000$ K. We normalized the blackbody energy distribution to the observed spectrum at 8 μm, i.e., we are assuming that at 8 μm, we are observing emission from the photosphere only. This is a reasonable approximation for spectra with weak emission features; but it underestimates the excess for spectra with strong emission features since models for these have shown that the CDS can contribute significantly to the flux at 8 μm. Varying the adopted photospheric temperature from 2000 K to 3000 K produced an uncertainty in the derived 8–22 μm excess by about 10%. However, the uncertainties in the excesses are as much as 20%–30% for stars with low S/N LRS (those with 8 μm fluxes of < 15 Jy) since it is difficult to determine the continuum temperature. It is also difficult to define weak emission features in these noisy spectra.

Figure 4 shows the 8–22 μm excess plotted against the period for Mira variables (*open circles*) and SR variables (*crosses*). A clear trend can be seen for Mira variables. S, MS, and SC Mira variables with $P > 400^d$ have excesses that are larger than 40% and Mira variables with $P < 370^d$ have excesses usually less than about 15%. In the 370^d–400^d range, the amount of excess for Mira variables rises sharply. No trend with period is observed for the SR variables except that the few SRs with periods between 300 and 390^d show the same amount of excess as the Mira variables in this period range suggesting a fundamental similarity between these SR stars and the Mira variables. The major anomaly is TT CMa which has a strong 10 μm silicate emission feature and a very large excess and may be part of a binary system. Jura (1988), who correlated the ratio of the 2 μm IRC flux to the 25 μm *IRAS* flux versus period, reached a similar conclusion that the 25 μm excess for all S stars increases sharply for stars with $P > \sim 360$ days.

Figure 5 shows that our 8–22 μm excesses correlate fairly well with the mass-loss rates for S stars as calculated by Jura (1988) for all types of stars—Mira, SR, Lb variables and non-variables. On the other hand, only for Mira variables do we find that the mass-loss rate correlates with period (Fig. 6). For mass-loss rates $< 5 \times 10^{-8}$ $M_\odot$ yr^{-1}, no dust grain emission features are observed and only W Cet and V441 Cyg show a very weak 8–22 μm excess. However, the presence and strength of dust grain emission features in the 8–22 μm region do not appear to correlate with mass-loss rate. Whereas the mass loss rates varies by a factor of 100 among the Mira MS and S stars, the contrast of the emission feature varies, seemingly randomly, by only a factor of 2. For example, W Aql, the star with the largest mass-loss rate of 4.5×10^{-6} $M_\odot$ yr^{-1} has one of the weakest emission features ($C_T = 16$). Hence it appears that the amount of material emitting continuum radiation in the CDS is related to the mass-loss rate (as expected), whereas the presence and strength of grain emission features appear not to be driven directly by the mass-loss rate.

Jura (1986) found that C star Mira variables with $P > 400^d$ tend to have larger mass-loss rates. Hence, it appears that mass outflow increases significantly for S, MS, SC, and C Mira variables with $P > 370$ days. On the other hand, DeGioia-

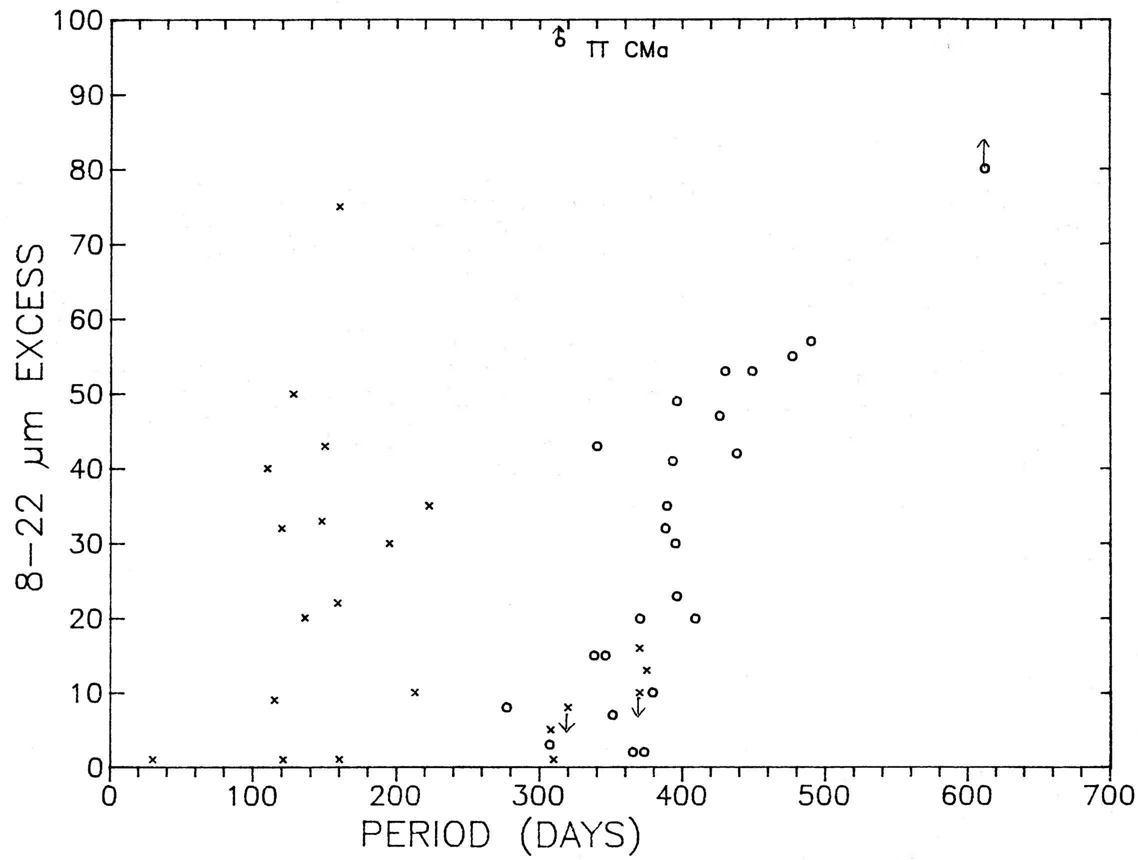

FIG. 4.—The 8–22 μm excess is plotted vs. the period of MS, S, and SC Miras (*open circles*) and SR variables (*crosses*). The rapid onset of excess emission for Miras with periods > 370 days can be seen. No correlation appears to be present for the SR variables. Arrows on the data points indicate upper and lower limits.

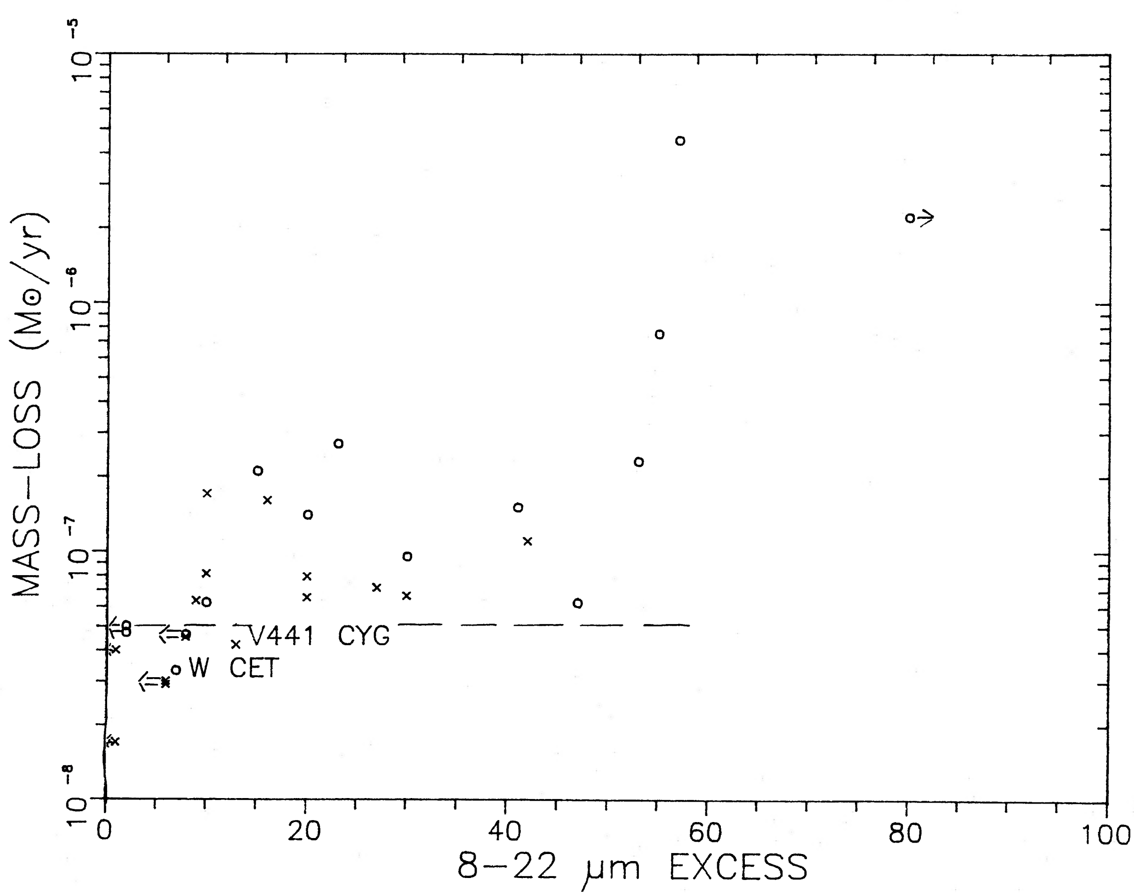

FIG. 5.—The mass-loss rate of Miras (*open circles*) and SR and Lb variables (*crosses*) is plotted vs. their 8–22 μm excess. Stars with mass-loss rates of $< 5 \times 10^{-8}$ $M_{\odot}$ yr show no emission features in their spectra, and only W Cet and V441 Cyg show a weak excess. Arrows on the data points indicate upper and lower limits.

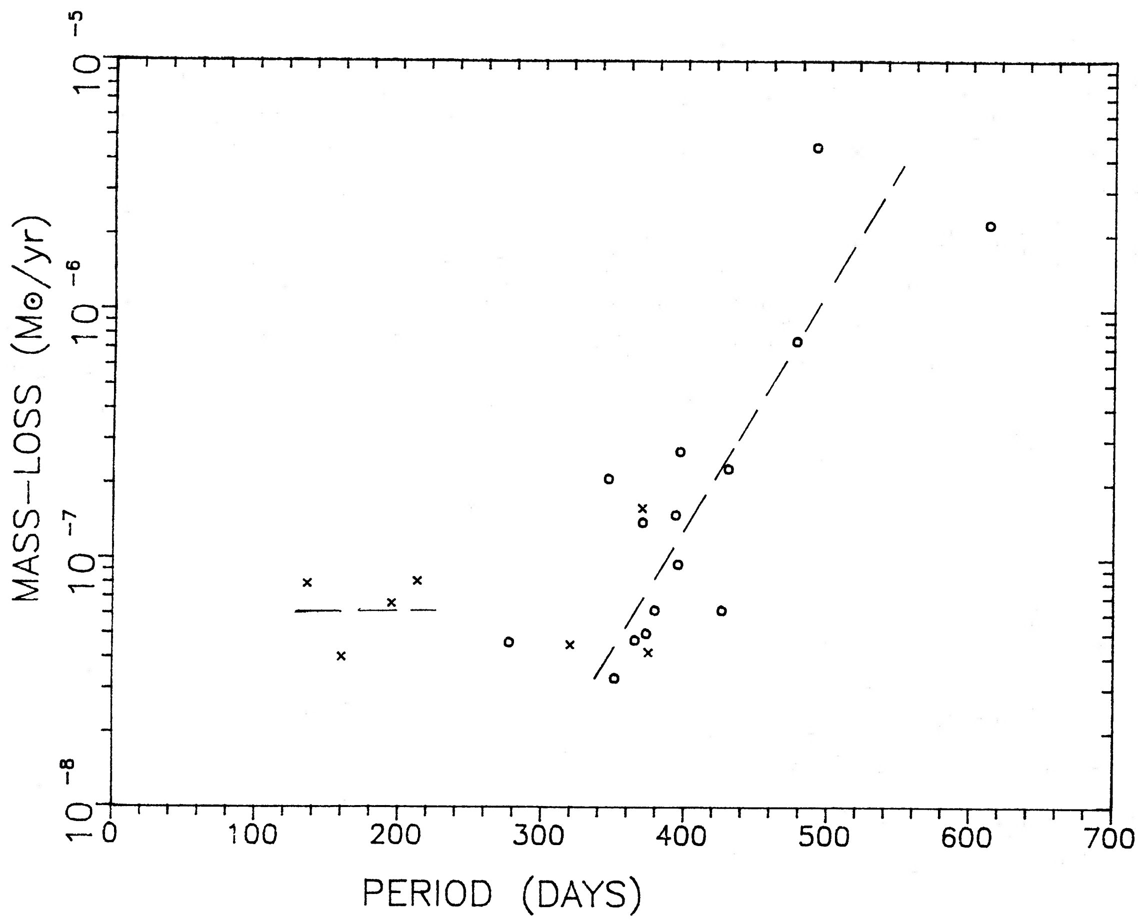

FIG. 6.—The mass-loss rates of Miras (*open circles*) and SR variables (*crosses*) are plotted vs. their period. The mass-loss rate increases with period for Miras but shows no correlation with period for the SR variables.

Eastwood *et al.* (1981) observed an increase in the infrared excess for M star Mira variables with $P > 200$ days, i.e., for significantly shorter periods than for the more evolved stars. Whether or not the same correlation between period and mass loss rate exists for M Mira variables as for the more evolved stars should be investigated. Also, the radioactive element technetium, as a tracer of the third dredge-up, is found predominantly in M Mira variables with $P > 300^d$ (Little, Little-Marenin, and Bauer 1987). It is likely that the onset of the third dredge-up should produce an increase in mass-loss rate and infrared excess and should be observed for M Mira variables with $P > 300^d$, rather than for $P > 200^d$ as suggested by DeGioia-Eastwood *et al.* (1981).

Whereas four out of 23 (17%) of S, MS, and SC Mira variables have no 8–22 μm excesses or emission features, we find that only six out of 460 (less than 2%) LRS spectra of ordinary M Miras have featureless photospheric continua. The significantly smaller percentage of M star Miras with featureless continua may indicate that for M Miras the mass-loss rate or the transparency of CDS or some other factor differs significantly from that of MS, S, and SC Miras. The M Mira variables as well as the MS and S Mira variables without emission features have $P < 400^d$.

VII. CONCLUSIONS

We find that the emission features of the MS, S, and SC stars show a progression of features with spectral class. Features in MS stars range from the 10 μm silicate emission and three-component feature found in M star spectra, to the 10.8 μm S star feature. Strong S stars show a characteristic emission feature which peaks in the 10.3–11 μm range, and SC stars show features characteristic of S and C stars. A few MS and S stars show a weak, broad 9–15 μm emission feature often found in M star LRS spectra. The exact nature of the carrier of the three-component, the 10.3–11 μm feature and the broad 9–15 μm feature remains unidentified. However, the different emission features are likely to be related to the changes in photospheric composition observed in stars that evolve from M stars with C/O < 1 to C stars with C/O > 1 accompanied by a dramatic increase in *s*-process abundances. Since more and more of the available oxygen is tied up in CO as stars evolve from $M \rightarrow$ S stars and *s*-process elements become more available, we propose that dust grains with different compositions are produced in the CDS. The three-component feature and the typical 10.8 μm S star feature are also found in a few stars classified as M stars. Whether or not these stars are related in their photospheric composition to the MS and S stars needs to be investigated.

The 8–22 μm emission excess correlates with the period of pulsation for the Mira variables in our sample showing a dramatic increase in emission excess for periods between 370 and 400 days. No correlation between the period and 8–22 μm excess of SR variables is found. The excess emission for all types of variables (Mira, SR, and Lb) and nonvariables correlates fairly well with their mass-loss rates.

I. R. L.-M. would like to thank the Air Force Systems Command for a University Resident Research Fellowship to the Air Force Geophysics Laboratory, OPC. S. J. L. thanks Bentley College for an Assigned Time grant for research. We would like to thank the referee for suggestions on improving the paper.

REFERENCES

Allen, D. S., Hyland, A. R., Longmore, A. J., Caswell, J. L., Goss, W. M., and Haynes, R. F. 1977, *Ap. J.*, **217**, 108.
Benson, P. J., and Little-Marenin, I. R. 1987, *Ap. J. (Letters)*, **316**, L37.
Bode, M. F., Evans, A., Whittet, D. C. B., Aitken, D. K., Roche, P. R., and Whitmore, B. 1984, *M.N.R.A.S.*, **207**, 897.
Catchpole, R. M., and Feast, M. W. 1971, *M.N.R.A.S.*, **154**, 197.
DeGioia-Eastwood, K., Hackwell, J. A., Grasdalen, G. L., and Gehrz, R. D. 1981, *Ap. J. (Letters)*, **245**, L75.
Dominy, J. F., and Wallerstein, G. 1986, *Ap. J.*, **310**, 371.
Dominy, J. F., Wallerstein, G., and Suntzeff, N. B. 1986, *Ap. J.*, **300**, 325.
IRAS Catalogs and Atlases Explanatory Supplement 1984, C. A. Beichman, G. Neugebauer, H. J. Habing, T. E. Clegg, and T. J. Chester (Washington, DC: US Government Printing Office).
Gal, O., de Muizon, M., Papoular, R., and Pegourie, B. 1987, *Astr. Ap.*, **183**, 29.
Gehrz, R. D., Ney, E. P., Grasdalen, G. L., Hackwell, J. A., and Thronson H. A., Jr. 1984, *Ap. J.*, **281**, 303.
Hoffleit, D., and Jaschek, C. 1982, *Bright Star Catalogue* (New Haven: Yale University Press).
Iben, I., Jr., and Renzini, A. 1983, *Ann. Rev. Astr. Ap.*, **21**, 271.
IRAS Science Working Group. 1986, *Astr. Ap. Suppl.*, **65**, 607.
Jura, M. 1986, *Ap. J.*, **303**, 327.
———. 1988, *Ap. J. Suppl.*, **66**, 33.
Keenan, P. C., and Boeshaar, P. C. 1980, *Ap. J. Suppl.*, **43**, 379.
Keenan, P. C., Garrison, R. F., and Deutsch, A. J. 1974, *Ap. J. Suppl.*, **28**, 271.
Kholopov, P. N., ed. 1985, *General Catalog of Variable Stars* (4th ed.; Moscow: Nauka).
Lambert, D. L., Gustafsson, B., Eriksson, K., and Hinkle, K. H. 1986, *Ap. J. Suppl.*, **62**, 373.
Little, S. J., Little-Marenin, I. R., and Bauer, W. H. 1987, *A.J.*, **94**, 981.
Little, S. J., Little-Marenin, I. R., and Price, S. D. 1987, in *Cool Stars, Stellar Systems, and the Sun*, ed. J. L. Linsky and R. Stencel (Heidelberg: Springer Verlag), p. 396.
Little-Marenin, I. R., Benson, P. J., and Dickinson, D. F. 1988, *Ap. J.*, **330**, 828.
Little-Marenin, I. R., Benson, P. J., and Little, S. J. 1987, *Cool Stars, Stellar Systems and the Sun*, ed. J. L. Linsky and R. Stencel (Heidelberg: Springer Verlag),p. 377.
Little-Marenin, I. R., Little, S. J., and Price, S. D. 1986, NASA Tech. Memo. 88342, p. 137.
Mathews, G. J., Takahashi, K., Ward, R. A., and Howard, W. H. 1986, *Ap. J.*, **302**, 410.
Neugebauer, G., and Leighton, R. B. 1969, *Two Micron Sky Survey—A Preliminary Catalog* (NASA SP-3047).
Nuth, J. A., III, Donn, B., and Nelson, R. 1986, *Ap. J. (Letters)*, **310**, L82.
Smith, V. V., and Lambert, D. L. 1985, *Ap. J.*, **294**, 326.
———. 1986, *Ap. J.*, **311**, 843.
Smith, V. V., and Wallerstein, G. 1983, *Ap. J.*, **273**, 742.
Snijders, M. A. J., Batt, T. J., Seaton, M. J., Blades, J. C., and Morton, D. C. 1984, *M.N.R.A.S.*, **211**, 7P.
Stephenson, C. B. 1973, *Pub. Warner and Swasey Obs.*, Vol. **1**, No. 4.
———. 1984, *Pub. Warner and Swasey Obs.* Vol. **3**, No. 1.
Thomas, J. A., Robinson, G., and Hyland, A. R. 1976, *M.N.R.A.S.*, **174**, 711.
Utsumi, K. 1985, in *Cool Stars with Excesses of Heavy Elements*, ed. M. Jaschek and P. C. Keenan (Dordrecht: Reidel), p. 243.
Wallerstein, G., and Dominy, J. F. 1988, *Ap. J.*, **326**, 292.
Willems, F. J. 1987 Ph.D. thesis, University of Amsterdam.
Wing, R. F., and Yorka, S. B. 1977, *M.N.R.A.S.*, **178**, 383.
Winters, R. R., and Macklin, R. L. 1987, *Ap. J.*, **313**, 808.
Wood, P. R. 1985, in *Cool Stars with Excesses of Heavy Elements*, ed. M. Jaschek and P. C. Keenan (Dordrecht: Reidel), p. 357.
Zuckerman, B., and Dyck, M. H. 1986, *Ap. J.*, **311**, 345.

STEPHEN J. LITTLE: Department of Natural Sciences, Bentley College, Waltham, MA 02254

I. R. LITTLE-MARENIN: Whitin Observatory, Wellesley College, Wellesley, MA 02181